Distributed Temperature Control for Safer Electric Vehicles

AURELIA DITTO, CEDRIC PAYAN, CELINE BONNAUD
and CLEMENT WEICK

ABSTRACT

As the adoption of electric vehicles continues to accelerate, managing the risks associated with battery technology has become critical. To ensure the safety of people and goods, it is essential to secure battery packs throughout their whole lifecycle, during charging, discharging, logistic and storage phases. However, current battery packs, which must constantly evolve to meet demands for reduced weight, volume, and cost in a competitive market, often underestimate an essential parameter: temperature reading. Temperature monitoring is a key element of battery health, yet it is typically performed at only a few points on the pack, limiting the reliability of the diagnostic. The present study proposes a novel approach based on time-domain reflectometry (TDR) to achieve real-time, distributed temperature monitoring along a single cable sensor. While optical fibbers approaches are discussed in the literature, TDR methods present easier integration, cost-efficiency, robustness, and can be installed with existing battery cables. The possibility of using readily available components such as coaxial cables and time-domain reflectometers with advanced signal processing techniques enables accurate temperature measurement. The first results comprising calibration experiments for various coaxial cable and validated temperature measurements over a range of zero to five meters. Using high-frequency signals, hot spots were detected with a precision of three centimeters, which is ideal for identifying overheating cells in a battery pack. Furthermore, the system can operate across a broad temperature range, including sub-zero environments and up to a hundred degrees, which is the range for battery surveillance. This innovative solution presents a promising path forward in Structural Health Monitoring, paving the way for safer and more reliable electric vehicle batteries.

Aurélia Ditto, PhD Student, Email: aurelia.ditto@cea.fr. Aix Marseille Univ, CNRS, Centrale Med, LMA UMR 7031, Marseille, France
Cédric Payan, PhD, Email: cedric.payan@univ-amu.fr. Aix Marseille Univ, CNRS, Centrale Med, LMA UMR 7031, Marseille, France
Céline Bonnaud, PhD, Email: celine.bonnaud@cea.fr. Univ. Grenoble Alpes, CEA, LITEN, DEHT, 38000 Grenoble, France
Cédric Payan, PhD, Email: clement.weick@cea.fr. Univ. Grenoble Alpes, CEA, LITEN, DEHT, 38000 Grenoble, France

INTRODUCTION

The era of electric vehicles began in the early 2010s. Since then, their performance has continuously improved in terms of capacity, charging time, lifespan, durability and safety. These improvements, powered by growing awareness of the challenges related to climate change and the need to decarbonize road transport, have contributed to the increase in electric vehicle sales. Unfortunately, the growth of this sector brings new risks associated with lithium-ion batteries. Indeed, if these batteries are used outside technical specifications or if they experience failures, they can catch fire or explode. The significance and frequency of these damages stem from the fact that a battery fire is difficult to contain because the associated chemical reaction is self-sustaining and exothermic. In most case, a battery fire is caused by the thermal runaway of a cell, which occurs because of event failures such as mechanical degradation of the cell, electrolyte leakage, short circuits, overcharging or overheating. When a cell undergoes thermal runaway, its temperature increases significantly, generating a hot spot, and the thermal runaway spreads to neighboring cells. In this context, close monitoring of the temperature in a lithium-ion battery is essential. Currently, this parameter is measured arbitrarily, sometimes just at few points within the battery which delays detection of an event and worsens the consequences of a failure. Most of the time, thermistors are used for their low price and simplicity [1] even if a large number of thermocouples will be more efficient to cover a larger monitoring area.

There are methods available to detect hot spots or measure temperatures in a distributed manner, such as thermography or thermal camera [2,3]. However, these technics require being at distance from the inspected object and cannot be integrated into a battery pack. Fiber optic sensors are commonly used in literature as distributed sensors [4] due to their effectiveness over long distances, but they are fragile because of the silica they contain which makes them not a good candidate for integration in a battery pack [5].

The present works based on Time Domain Reflectometry (TDR) measurement propose a method for integrating continuous and distributed temperature measurement directly into the battery from its design phase to enhance its safety by detecting an event at an early stage. This solution can be easily integrated into a battery pack thanks to the variety of coaxial cable diameters and it enables a single measurement to read temperature of all the cells.

Time Domain Reflectometry (TDR) is a well-known measurement technique used to analyse the characteristics of a circuits, particularly impedance, faults or changes in cables and transmission lines. Since the early 2000s, Tang *et al.* laid the foundations for the use of a coaxial cable and TDR to measure strain [6]. The use of this technique to study changes in a medium has been widely researched since then, especially for measuring deformations [7–10]. In 2023, Taillade *et al.* developed a method for monitoring concrete structures and demonstrated that TDR is as effective as optical fiber for detecting early signs of cracks and locating structural defects while being more robust [6]. A coaxial cable is connected to a Vector Network Analyzer (VNA) used here as a TDR to measure the electrical impedance or S11 parameter.

$$S11 = \frac{Z - Z_0}{Z + Z_0} \tag{1}$$

Z0 is the internal impedance of the TDR and Z is the electrical impedance of the coaxial cable.

In 2018 and 2019, Cheng *et al.* [11] et Zhu *et al.* [12] presented methods for detecting temperature variations by measuring the S11 parameter on an unmodified coaxial cable. Using a signal processing technique based on cross-correlation, the signals before and after heating are compared and temperature measurement are verified on cable segments of fifty centimeters. In a coaxial cable, the electromagnetic waves generated by TDR propagate through the dielectric insulator. The propagation speed of these waves depends on the dielectric permittivity of the material, which is not constant. The permittivity varies with temperature.

$$V_f = \frac{c}{\sqrt{\epsilon}} \tag{2}$$

Vf is the propagation speed in the cable, which represents the speed of electromagnetic wave propagation in the cable, c is the speed of the light in a vacuum 3^e8 m/s and ϵ is the denotes the dielectric permittivity of the insulating material.

The TDR used in this study is a Copper Mountain R60 model, capable of performing frequency sweeps from 0 to 6 GHz. The associated wavelength (λ) depends on the dielectric permittivity of material and the maximum frequency of the device (f).

$$\lambda = \frac{c}{\sqrt{\epsilon} * f} \tag{3}$$

In the case of a coaxial cable with polyethylene as the dielectric material and the R60 VNA, the theoretical wavelength is 3 cm at temperature of 25 degrees Celsius. This work uses the TDR's advantage of being able to measure differences in impedance. When the temperature of the environment changes, thermal expansion occurs in the cable, primarily due to the expansion of the dielectric material, along with a variation of the dielectric permittivity of the insulator. In the case of polyethylene, its dielectric permittivity decreases as the temperature increase [11].

These properties are used in the present works for both distributed temperature measurement and hot spots detection within a battery.

MATERIALS AND METHODS

DISTRIBUTED TEMPERATURE MEASUREMENT

To monitor temperature effectively using distributed temperature measurement, a first phase of correlation between TDR measurements and temperature has to be performed. This phase allows for correlating the S11 parameter values with temperatures. A two-and-a-half-meter long RG58 coaxial cable is placed in an oven and equipped with

two thermocouples. It is at room temperature (25 degrees Celsius) from 0 to 0.5 meter and it is in the oven from 0.5 to 2 meters as shown in Figure 1.

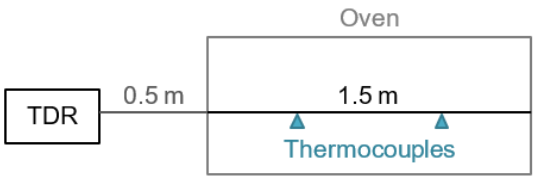

Figure 1. Correlation Setup

The oven is programmed to perform seven temperatures steps, ranging from 30 to 60 degrees Celsius in 5 degrees increments. Each step lasts ten minutes to ensure complete temperature homogenization inside the chamber and around the cable. Initial data from the TDR is recorded at the reference room temperature of 25 degrees Celsius and then measurements are taken at each step after the temperature has fully stabilized inside the chamber. The recorded data corresponds to the S11 parameter values as a function of the distance along the coaxial cable. By applying the equation 1, the impedance at each point is calculated. Then, each impedance is compared to the reference impedance at the temperature of 25 degrees Celsius.

By averaging the impedances at each point along the cable, from 0.5 to 2 meters, for each temperature level, a correlation graph is obtained, as shown in Figure 2. This graph allows the determination of the impedance corresponding to a specific section of cable between 0.5 to 2 meters long.

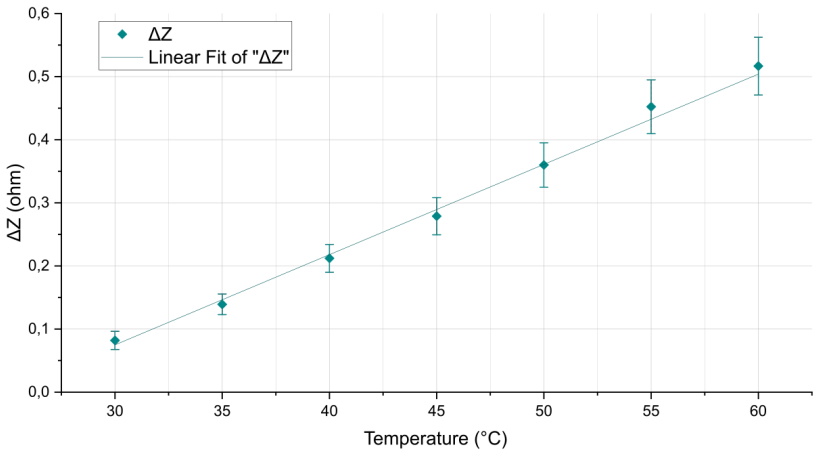

Figure 2. Temperature / ΔZ correlation graph for RG58 ∅6 mm coaxial cable (lenght 0.5 to 2 meters)

The coefficient of determination (R^2) is 0,9963, confirming a strong linear correlation between temperature and ΔZ. The standard deviation increases with temperature which may be attributed to 1) temperature inhomogeneities within the oven and along

the cable, 2) structural imperfections inherent to the cable used and 3) the loss of information at high temperature.

The temperature and the impedance can be related by applying this equation. This method is applicable to all types of coaxial cable but it can be affected by the quality of the cable. A new correlation has to be made for each different cable before using it for distributed temperature measurement. To validate this method, the 2.5-meters cable is fixed to a twelve-centimeters hot plate as shown in Figure 3.

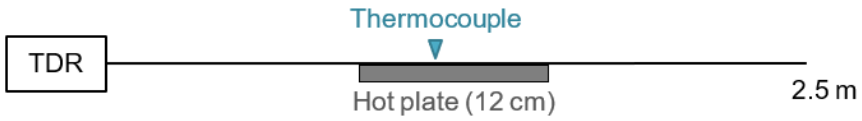

Figure 3. 12 cm hot plate on 2.5 m RG58 coaxial cable

The temperature is measured and recorded using a thermocouple after height minutes of stabilization at 40 °C and 50 °C and serves as reference. Then, the TDR data is recorded to correlate with the temperature. The results are presented in results section.

HOT SPOT DETECTION

The integration of a coaxial cable into a battery module must take into account weight and space constraints. For hot spot detection, a RG403 coaxial cable with a PTFE (Polytetrafluoroethylene) dielectric material with a 2.1 millimeters diameter has been selected. The theoretical wavelength of this material at a frequency of 6 GHz is 3.3 centimeters. The method to obtain the graph is identical to the method describe in Section **??**. A support structure is used to position the heating cells and the mimic cells both 18650 format. The mimic cells are made up of a casing only. The heating cells are made following the process described by Li *et al.* [13]. The coaxial cable is arranged so that each cell is in contact with a portion of the cable.

A first test is conducted with only one heating cell positioned at 0.5 m along the coaxial cable and twenty-nine dummy cells to demonstrate the feasibility of a hot spot detection as shown in Figure 4.

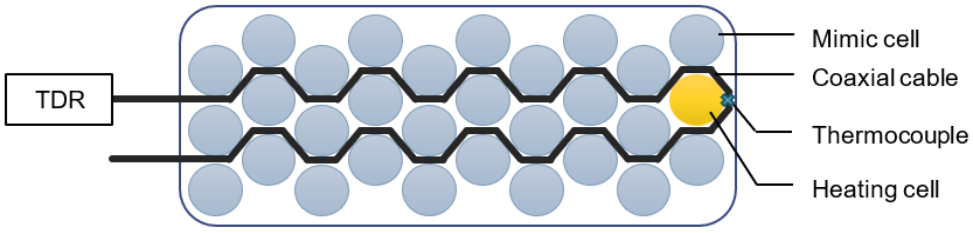

Figure 4. Hot spot setup with one heating cell positioned at 0.5 meter

A second test is conducted with four heating cells and twenty-six mimic cells. The

heating cells are distributed in the support such that cell 1 is at 14 cm along the cable, cell 2 is at 22 cm and at 40 cm, cell 3 is at 29 cm and cell 4 is at 14 cm and at 47 cm. The heating cells are equipped with thermocouples to monitor the surface temperature as shown in Figure 5.

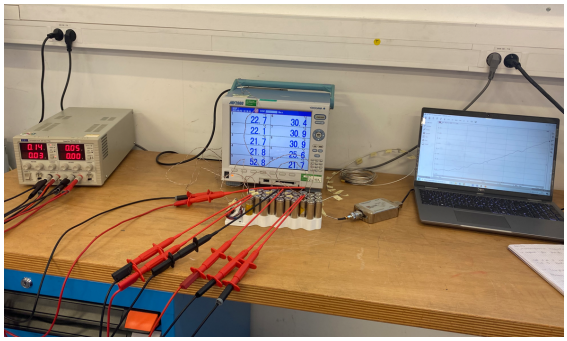

Figure 5. Picture of hot spot setup with four heating cells

The data from the TDR and thermocouples were recorded thirteen times, starting from t0, before the heating began, which represent the reference point, up to t12, when the heating was completely stopped. The temperatures T1, T2, T3 and T4 reported in Table II correspond to the temperatures recorded by the thermocouples on the heating cells respectively 1, 2, 3 and 4. The "Time" column refers to the elapsed time from t0 at the moment of measurement. The measurement speed is limited by the intermediate frequency bandwidth (IFBW); in this case the measurement was made with a 3 kHz IFBW.

RESULTS

DISTRIBUTED TEMPERATURE MEASUREMENT

The Figure 6 shows the ΔZ Hot-plate recording by the TDR after height minutes of temperature stabilization.

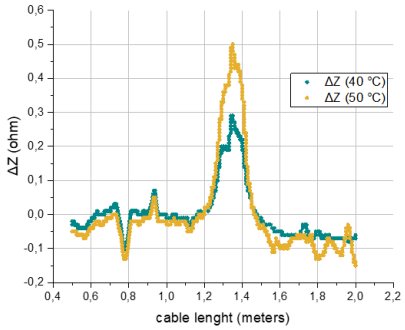

Figure 6. ΔZ hot plate at 1.3 meters on the cable

The ΔZ values over portion of cable on which the heating plate is placed are averaging to obtain the coefficients ΔZ Hot-plate. The TABLE I lists the temperatures measured with the thermocouple, the ΔZ theoretical obtain with the correlation graph, the ΔZ Hot-plate and the deviation which is the percentage difference between ΔZ theoretical and ΔZ Hot-plate.

TABLE I. COMPARISON OF THEORETICAL AND HOT-PLATE ΔZ VALUES

Temperature °C	**ΔZ Theoretical ohm**	**ΔZ Hot-plate ohm**	**Deviation %**
40	0.21	0.22	4.76
50	0.36	0.38	5.56

With a deviation of less 10 %, these two results indicate a correlation between the ΔZ value measured using TDR and the temperature measured with a thermocouple. Additional measurements are necessary to confirm and validate the correlation. This correlation is only valid as long as the cable remains in its original conditions, meaning it has not suffered mechanical degradation such as deformation, puncturing or compressing.

HOT SPOTS DETECTION

In Figure 7, the peak impedance variation is centred around 0.5 cm, corresponding precisely to the position of the hot spot simulated by the assembly described in Figure 4.

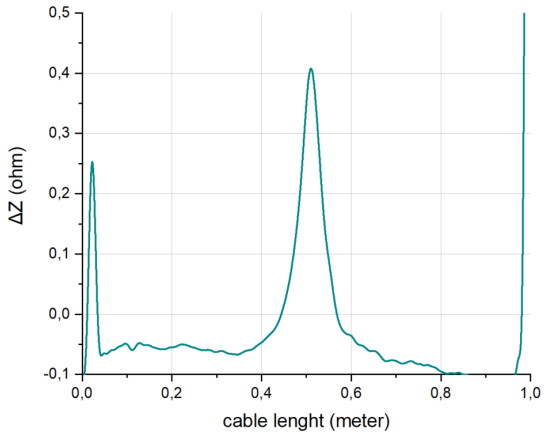

Figure 7. Hot spot graph, coaxial cable ∅ 2.1 mm, heating cell at 0.5 meter along the cable, heating spot temperature 70 °C for two minutes

This method allows for precise fault location within a battery. The 3.3 centimeters wavelength at 6 GHz enables identification of the fault cell among thirty cells, provided that the coordinates along the cable for cell are known. The amplitude ΔZ does not correspond to the amplitude value obtaining with the correlation equation in Materials

and Methods section. This is because the wavelength of 3.3 centimeters at 6 GHz leads to amplitude limitation for hot spot smaller than 3.3 centimeters.

The TABLE II contains data from thermocouples (T1, T2, T3, T4) extracted during the second test for multiple hot spots detection. Five results are presented, t0, t1 which corresponds to ten degrees increase, t6 which is an intermediate measurement, and t11 and t12 separated by twenty seconds.

TABLE II. TIME AND TEMPERATURE MEASURMENT, MULTIPLE HOT SPOTS SETUP

	Time min:s	**T1 °C**	**T2 °C**	**T3 °C**	**T4 °C**
t0	14:16	22.3	22.1	21.6	22.5
t1	17:00	31.2	30.4	30.4	32.2
t6	20:20	59.7	53.9	56.1	58.8
t11	22:10	81.2	71.3	76	79.1
t12	22:30	85.4	74.8	79.7	83

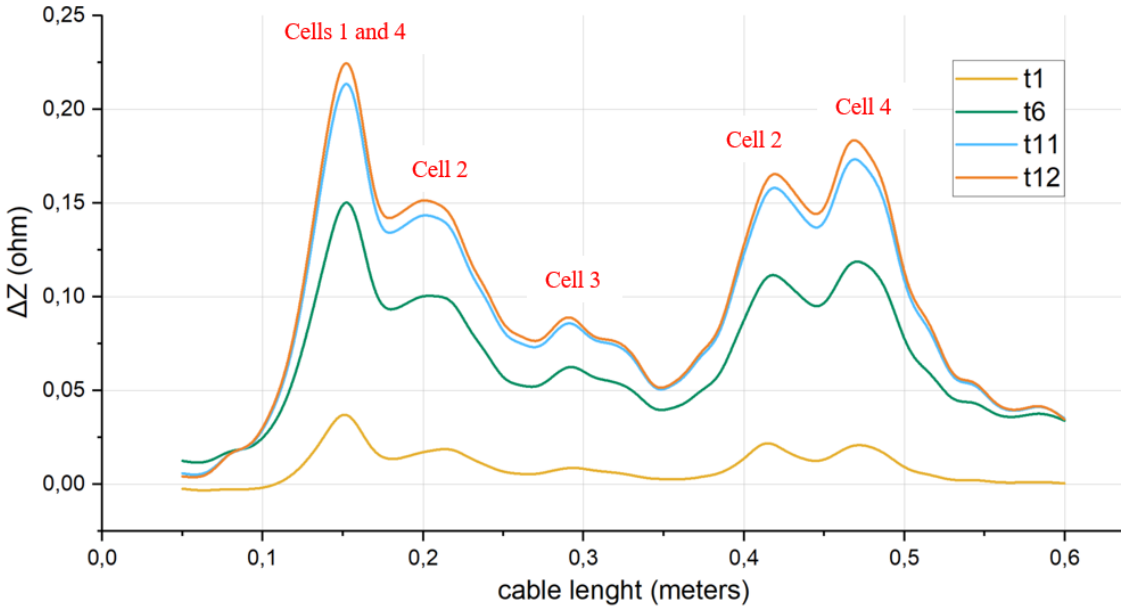

Figure 8. Hot spots graph, coaxial cable ∅ 2.1 mm, four heating cells

Each heating cell has unique graphical signature visible on Figure 8 that corresponds to its position along the cable. For instance, in case of heating, cell 1 will cause a local impedance increase at 14 centimeters while cell 4 will cause two increases, at 14 and 47 centimeters. This method is promising for the identification of a faulty cells based on their distinctive signatures.

CONCLUSION

The first part of this work focused on the correlation between ΔZ and temperature, demonstrated the potential for ambient temperature measurement using a coaxial cable and Time Domain Reflectometry. The next phase of the study will explore the influence of cable length on the measurement. The second part of this work demonstrated the feasibility of detecting a hotspot in a system simulating a classic battery module, as well as the potential to identify the faulty cell based by analysing its graphical signature. The upcoming work will focus on evaluating the sensor's response within an actual battery module. It is also essential to study the relationship between the ΔZ measured at a hotspot and the ΔZ obtained during calibration, in order to establish a correlation and thereby estimate the temperature of the hotspots. This work proposes to use a coaxial cable as a continuous temperature sensor in electric batteries. Connected to a TDR-mode device, it provides a simple reading of the module's operating temperature and the spatial identification of any hotspots. By checking that the battery is operating evenly under normal temperature conditions, safety and the state of health of the battery are increased.

REFERENCES

1. Zhao, Y., L. Geng, S. Shan, Z. Du, X. Hu, and X. Wei. "Review of sensor fault diagnosis and fault-tolerant control techniques of lithium-ion batteries for electric vehicles," 11(6):1447–1466, ISSN 2095-7564, doi:10.1016/j.jtte.2024.09.003.
2. M., C., J. K.v., S. T., and R. P.k. "Comprehensive experimental study of battery thermal management using single-phase liquid immersion cooling," 111:115445, ISSN 2352-152X, doi:10.1016/j.est.2025.115445.
3. Dileep, H., K. K. Jha, P. S. Mahapatra, and A. Pattamatta. 2024. "Thermal characterization of pouch cell using infrared thermography and electrochemical modelling for the Design of Effective Battery Thermal Management System," *Applied Energy*, 376:124301, doi:10.1016/j.apenergy.2024.124301.
4. Zhang, X., L. Long, W. Broere, and X. Bao. 2025. "Smart sensing of concrete crack using distributed fiber optics sensors: Current advances and perspectives," *Case Studies in Construction Materials*, 22, doi:10.1016/j.cscm.2025.e04493.
5. Bao, X. and L. Chen. "Recent Progress in Distributed Fiber Optic Sensors," 12(7):8601–8639, ISSN 1424-8220, doi:10.3390/s120708601.
6. Taillade, F., S. Michel-Ponnelle, B. Masson, M. Corbin, A. Courtois, and M. Galan. "Post-tension cables monitoring system," in *NDE NucCon 2023 - International Conference on Non-destructive Evaluation of Concrete in Nuclear Applications January 25-27, 2023, Espoo, Finland*.
7. Engl, M., W. Eurskens, and R. Weigel. "Comparison of time domain package characterization techniques using TDR and VNA," in *Proceedings of 6th Electronics Packaging Technology Conference (EPTC 2004) (IEEE Cat. No.04EX971)*, pp. 490–495, doi:10.1109/EPTC.2004.1396657.
8. Zhu, C. and J. Huang. "Coaxial Cable Sensing: Review and Perspective," 72(3), ISSN 0018-9480, 1557-9670, doi:10.1109/TMTT.2023.3305049.
9. Ong, R. and K. Cheong. "Non-destructive electrical test detection on copper wire micro-crack weld defect in semiconductor device," in *Proceedings of the IEEE/CPMT Interna-*

tional Electronics Manufacturing Technology (IEMT) Symposium, vol. 2016-November, ISBN 978-1-5090-3443-7, doi:10.1109/IEMT.2016.7761967.

10. Lu, Y., B. Yao, M. Wan, and J. Feng. "Time domain reflectometry technique for detecting the degradation of solder joints," in *ICRMS'2011 - Safety First, Reliability Primary: Proceedings of 2011 9th International Conference on Reliability, Maintainability and Safety*, ISBN 978-1-61284-664-4, pp. 395–397, doi:10.1109/ICRMS.2011.5979300.
11. Cheng, B., L. Hua, W. Zhu, Q. Zhang, J. Lei, and H. Xiao. "Distributed temperature sensing with unmodified coaxial cable based on random reflections in TDR signal," 30(1):015105, ISSN 0957-0233, 1361-6501, doi:10.1088/1361-6501/aaee4f.
12. Zhu, C., Y. Zhuang, Y. Chen, and J. Huang. "Truly Distributed Coaxial Cable Sensing Based on Random Inhomogeneities," 68(11):4600–4607, ISSN 0018-9456, 1557-9662, doi:10.1109/TIM.2018.2890327.
13. Li, W., S. Xiong, X. Zhou, W. Shi, C. Wang, X. Lin, and J. Cheng. "Design of Cylindrical Thermal Dummy Cell for Development of Lithium-Ion Battery Thermal Management System," 14(5):1357, ISSN 1996-1073, doi:10.3390/en14051357.